Electronic Supplementary Material (ESI) for Lab on a Chip.

Supporting Information

Separation and Dual Detection of Prostate Cancer Cells and Protein Biomarkers Using a Microchip Device

Wanfeng Huang, Chun-Li Chang, Norman D. Brault, Onur Gur, Zhe Wang, Shadia I. Jalal, Philip S. Low, Timothy L. Ratliff, Roberto Pili, and Cagri A. Savran

Contents:

S1. The single–chamber prototype and a comparison to the new device

Using a single-chamber prototype (Figure S1-A), we have previously reported a preliminary study in which both free-molecules and cells could be simultaneously captured on a glass slide.[1] However, due to the inability to separate the small free molecule-bead complexes from the larger cell-bead complexes and free beads, the ability to perform quantification was limited.

Figure S1-B shows several bright-field microscopic images illustrating this inadequacy. The left column of images is for the single-chamber prototype which contains a glass surface for capturing targets. The right column of images is for the new device that utilizes the micro-aperture chip containing an array of 6 μm holes. The top row reveals the appearance of an unused surface for each system. The middle row shows the results of an experiment in which 80 μg of only antibody-conjugated magnetic beads (incubated in culture media without cells present) were captured using each device. While the chamber containing the glass slide resulted in a roughened surface with large dark clusters of beads, the dual magnet mode[2] integrated with the micro-aperture chip led to a much cleaner surface with only a few very small bead aggregates (i.e. the four small dark spots in the image which represent the "worst" location on the chip surface). The bottom row shows the results of a similar experiment as that of the middle section but in the presence of target cells. For the single-chamber glass surface, the difficulty in visualizing captured cells in the presence of the large dark bead clusters combined with the significantly roughened surface from the free-bead background limited the accuracy of quantification (fluorescence detection and bright-field). This was mostly due to the difficulty of counting the numbers of cells present in the big clusters (or if there were any at all). Furthermore, there was the potential for the large bead aggregates to interfere with the quantification process by influencing the fluorescence signal, which also created problems for free-protein detection by masking some of the fluorescence output. The use of the dual-magnet mode was unable to break up the bead clusters. However, the dual-chamber system containing the micro-aperture chip successfully resolved these issues by separating the cell-bead complexes onto the top of the micro-aperture chip while allowing protein-bead complexes and free beads to pass through to the lower chamber. It should be noted that the cells appear dark due to being complexed with antibody-conjugated magnetic beads.

(A)

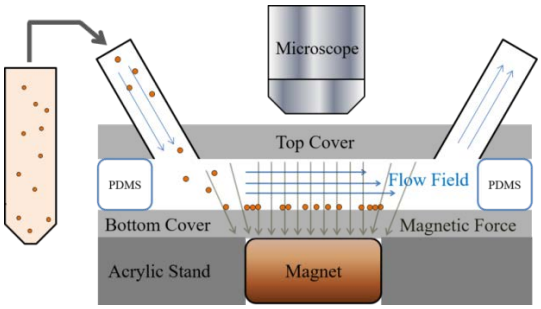

(B)

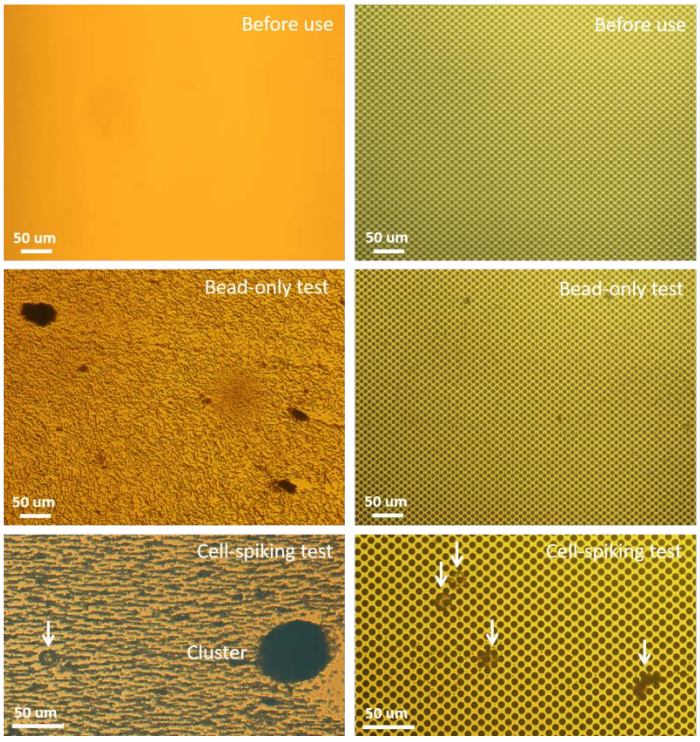

Figure S1. (A) Schematic diagram of the preliminary single-chamber system. (B) Bright-field images on the left are for the single-chamber prototype containing a glass slide (viewed from the top). Images on the right are for the dual chamber system in which the micro-aperture chip surface (viewed from the top) is presented. The micro-chip contains an array of ~6 µm diameter holes that appear dark. The top row of images corresponds to unused surfaces. The middle row shows the results of 80 µg of magnetic beads (incubated in culture media without cells) captured using both devices. The dark spots and roughened background for the glass chip are due to the beads, which contrast to the clear micro-aperture chip surface. The bottom row reveals the results of the same experiment as for the middle section but in the presence of target cells. Cells are identified with white arrows and appear dark due to being bound to antibody conjugated magnetic beads. The large cluster and bead-background on the glass surface limit the ability for accurate cell quantification.

S2. LNCaP and KB cell surface protein expression analysis

Antibody-tagged fluorescence labeling was used to study the expression of several antigens on LNCaP and KB cell surfaces. For LNCaP cells, these include EpCAM, PSMA and EGFR. For KB cells, only EpCAM and Folate Receptor (FR) were analyzed. Each surface marker was analyzed one at a time using the following generalized protocol. The cells were first released from the culture flask. After centrifugation, 10 μL of a single biotinylated polyclonal antibody (0.2 mg/mL) was introduced and incubated with the cells in 100 μL of culture media for 30 min. Another round of centrifugation was applied to remove free antibodies. Next, 100 μL of avidin-FITC (1:10 dilution in PBS) was added and incubated for 30 min. The extra fluorescent dye solution was then removed and the stained cells were observed under a fluorescence microscope. Representative fluorescence and bright-field images of cells are shown in Figure S2 (A). For each surface marker, the total fluorescence intensity per image was calculated and then normalized by the total number of cells from the bright-field image. The normalized value, the “Staining Ratio”, was used as a measure of the level of antigen expression as shown in Figure S2 (B) and (C) for LNCaP and KB cells, respectively. The control experiment was performed identically to that above, only without the addition of antibody.

(A)

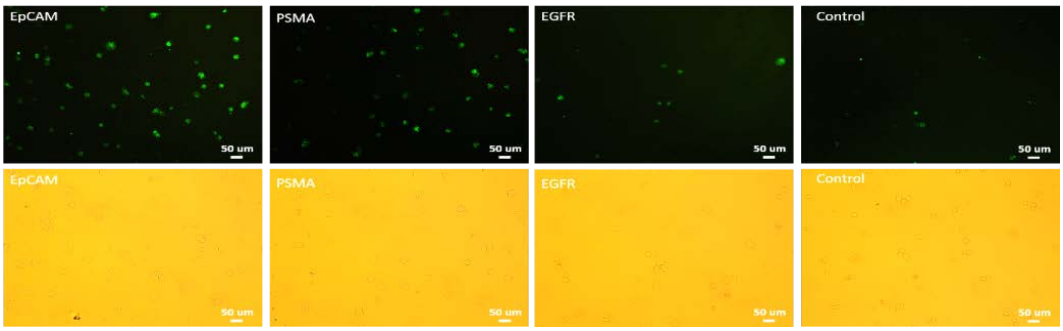

(B)

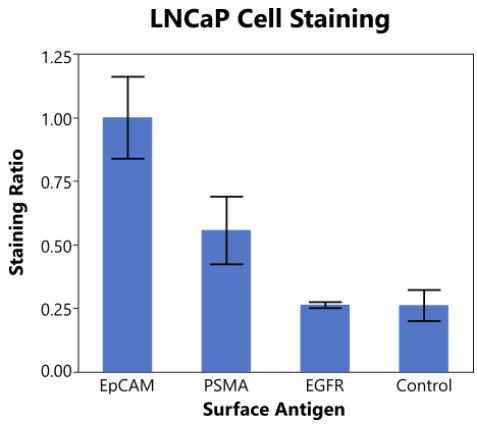

(C)

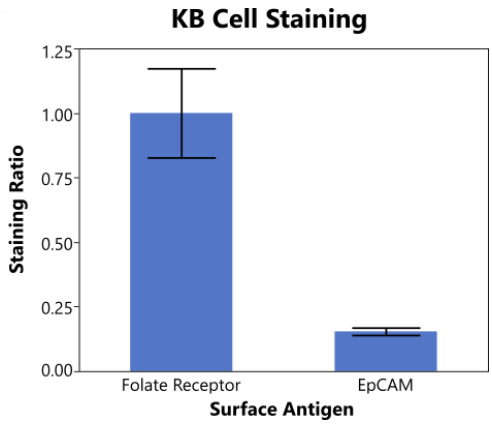

Figure S2. (A) Representative fluorescence (top) and bright-field (bottom) images of cells stained with biotinylated antibodies for several surface markers, with the former visualized via avidin-FITC. (B and C) Relative staining ratios for corresponding antigens expressed on LNCaP (B) and KB (C) cells. Error bars represents one standard deviation from three experiments.

S3. KB cell detection

KB cells, a cancer cell line which over-expresses Folate Receptor (FR), lacks PSMA, and only has a minor amount of EpCAM, were used as a negative control. Approximately 100 KB cells were first incubated with the anti-PSMA and anti-EpCAM bead mixture (i.e. 40 µg of each antibody conjugated bead) in culture media. The solution was then injected into the micro-aperture device and the detection yield was determined. The results showed that only ~9% of spiked KB cells were captured compared to ~95% of the LNCaP cells.

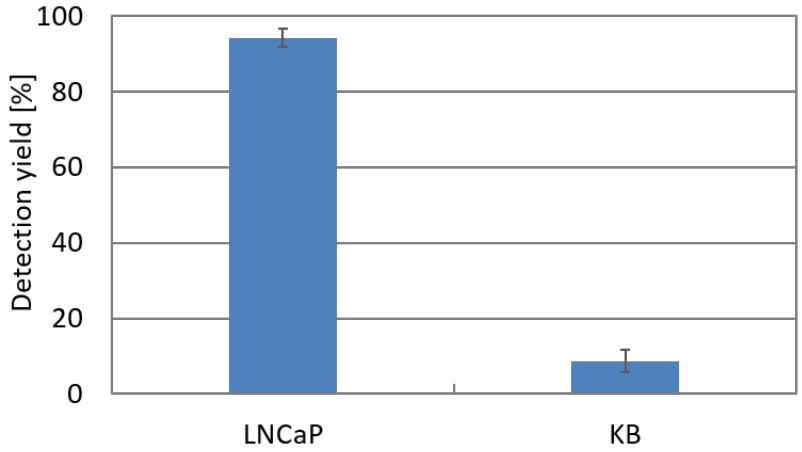

Figure S3. Detection yields of LNCaP and KB cells captured using the anti-PSMA and anti-EpCAM bead mixture spiked into cell culture media.

S4. Detection limit of PSMA from culture media

The intersection (red dot in Figure S4) of the fitted Langmuir Isotherm curve with the background-plus-three-standard-deviation line was used to determine the limit of detection (LOD) of PSMA spiked into culture media.

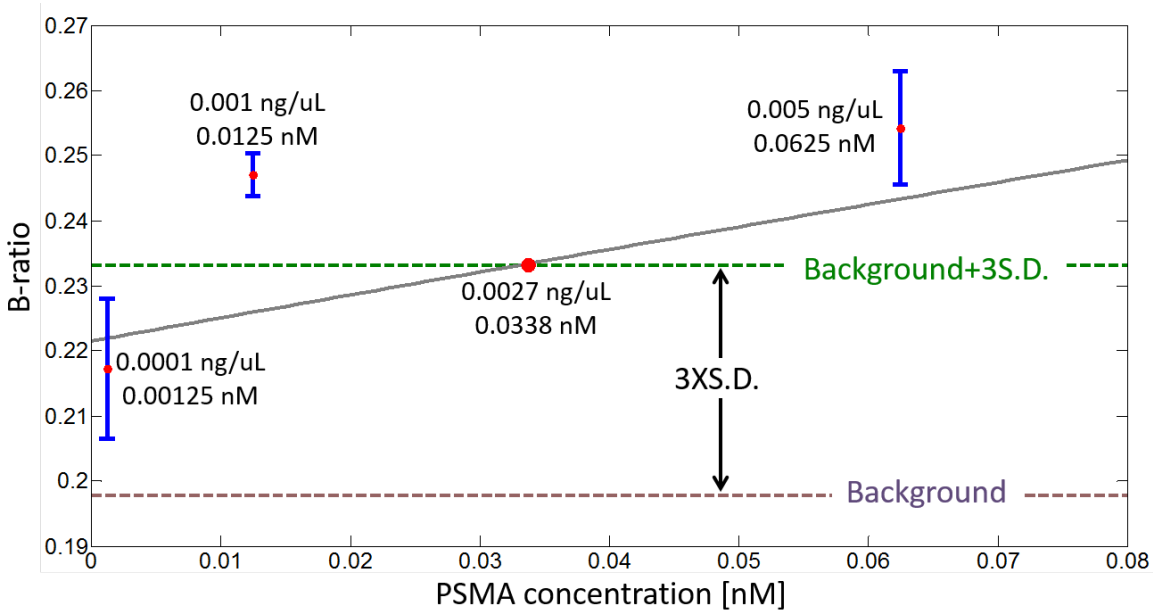

Figure S4. Detection limit of PSMA spiked into culture media in the absence of LNCaP cells.

S5. Influence of antibody-bead combinations on free-PSMA detection

Different combinations of antibody beads (anti-EpCAM, anti-PSMA plus anti-EpCAM, and anti-PSMA) were used to detect free-PSMA spiked into culture media in the absence of LNCaP cells. According to the results, anti-PSMA plays the dominant role in detecting the free-PSMA protein while the anti-EpCAM contribution is negligible.

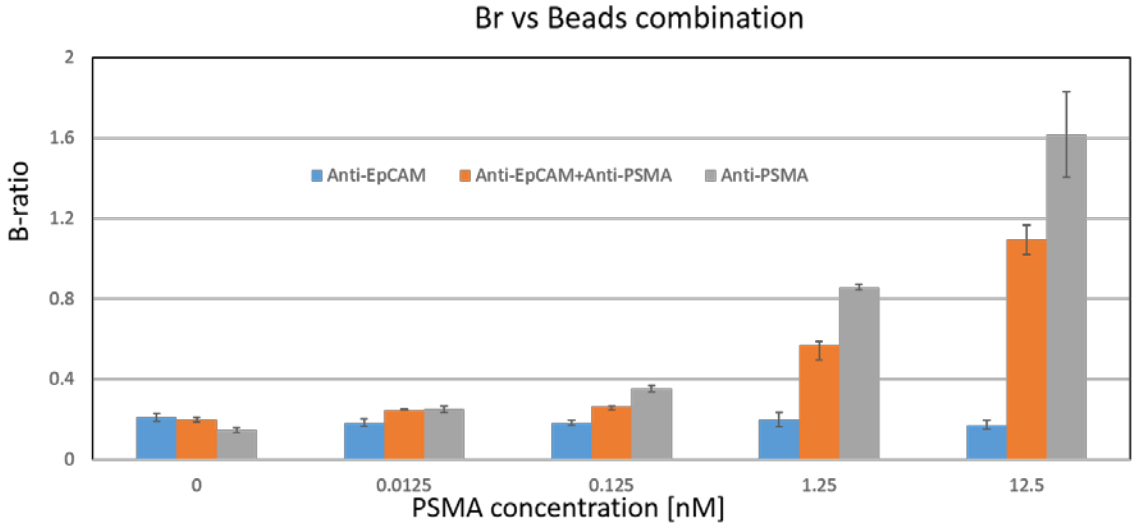

Figure S5. B-ratios of different combinations of antibody beads (anti-EpCAM, anti-PSMA plus anti-EpCAM, and anti-PSMA) for detecting multiple concentrations of PSMA (0 - 12.5 nM) spiked into culture media.

S6. Influence of LNCaP cell concentration on PSMA detection

Different numbers of LNCaP cells (0 – 80) were spiked into 1 mL of culture media while keeping the amount of free-PSMA added, held constant at 1.25 nM (100 ng/mL). For each experiment, the anti-PSMA and anti-EpCAM bead mixture was used for detection and the PSMA concentration was inferred from a standard curve (Figure 7 and Equation 1). The results (Figure S6) showed that the measured PSMA concentrations ranged from 0.96 – 1.33 nM (77 – 110 ng/mL). This demonstrates that the ability to capture free-protein targets is not significantly affected by the amount of target cells present, over the range expected for rare cells.[3-5]

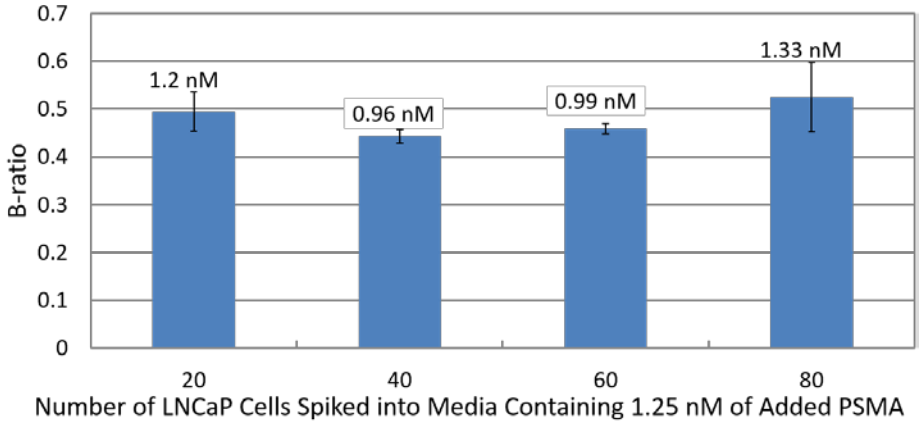

Figure S6. Measured PSMA concentrations (using Equation 1) which were concurrently detected from culture media samples containing different numbers of spiked LNCaP cells and 1.25 nM of added PSMA.

References:

1. W. Huang, C. L. Chang, B. D. Chan, S. I. Jalal, D. E. Matei, P. S. Low and C. A. Savran, *Anal. Chem.*, 2015, **87**, 10205-10212.
2. C. L. Chang, W. Huang, S. I. Jalal, B. D. Chan, A. Mahmood, S. Shahda, B. H. O'Neil, D. E. Matei and C. A. Savran, *Lab Chip*, 2015, **15**, 1677-1688.
3. D. C. Danila, M. Fleisher and H. I. Scher, *Clin. Cancer Res.*, 2011, **17**, 3903-3912.
4. S. Nagrath, L. V. Sequist, S. Maheswaran, D. W. Bell, D. Irimia, L. Ulkus, M. R. Smith, E. L. Kwak, S. Digumarthy, A. Muzikansky, P. Ryan, U. J. Balis, R. G. Tompkins, D. A. Haber and M. Toner, *Nature*, 2007, **450**, 1235-U1210.
5. S. L. Stott, C. H. Hsu, D. I. Tsukrov, M. Yu, D. T. Miyamoto, B. A. Waltman, S. M. Rothenberg, A. M. Shah, M. E. Smas, G. K. Korir, F. P. Floyd, A. J. Gilman, J. B. Lord, D. Winokur, S. Springer, D. Irimia, S. Nagrath, L. V. Sequist, R. J. Lee, K. J. Isselbacher, S. Maheswaran, D. A. Haber and M. Toner, *Proc. Natl. Acad. Sci. U. S. A.*, 2010, **107**, 18392-18397.